DALTON

Gold(III) and palladium(II) complexes of glycylglycyl-L-histidine: crystal structures of $[Au^{III}(Gly\text{-}Gly\text{-}L\text{-}His\text{-}H_{-2})]Cl\cdot H_2O$ and $[Pd^{II}(Gly\text{-}Gly\text{-}L\text{-}His\text{-}H_{-2})]\cdot 1.5H_2O$ and HisεNH deprotonation

Sabine L. Best,[a] Tapan K. Chattopadhyay,[b] Milos I. Djuran,[a] Rex A. Palmer,[b] Peter J. Sadler,*†[a] Imre Sóvágó[c] and Katalin Varnagy[c]

[a] *Department of Chemistry, Birkbeck College, University of London, Gordon House and Christopher Ingold Laboratories, 29 Gordon Square, London, UK WC1H 0PP*
[b] *Department of Crystallography, Birkbeck College, Malet Street, London, UK WC1E 7HX*
[c] *Department of Inorganic and Analytical Chemistry, Lajos Kossuth University, H-4010 Debrecen, Hungary*

Proton NMR studies show that $[AuCl_4]^-$ reacts slowly with glycylglycyl-L-histidine (Gly-Gly-L-His) ($t_{\frac{1}{2}}$ = 9.3 h at 310 K and pH* 2) in D_2O at pH* (meter reading) values as low as 1.5 to form the stable complex $[Au^{III}(Gly\text{-}Gly\text{-}L\text{-}His\text{-}H_{-2})]Cl\cdot H_2O$ **1** *via* one intermediate. Complex **1** is shown by X-ray crystallography to be square-planar with gold bound to the terminal NH_2 [Au–N 2.049(10) Å], two deprotonated amide nitrogens [Au–N^- 1.941(9), 2.006(10) Å] and HisδN [Au–N 2.038(9) Å] giving one six-membered and two five-membered chelate rings. At pH* 7 the reaction of $[AuCl_4]^-$ with Gly-Gly-L-His follows a different course, apparently involving the formation of Au^{III} cross-linked polymers. The anion $[PdCl_4]^{2-}$ reacts rapidly with Gly-Gly-L-His also at pH* 2, and forms a similar square-planar complex $[Pd^{II}(Gly\text{-}Gly\text{-}L\text{-}His\text{-}H_{-2})]\cdot 1.5H_2O$ **2** involving the terminal NH_2 [Pd–N 2.058(7) Å], two deprotonated amide nitrogens [Pd–N^- 1.943(7), 1.983(6) Å] and HisδN [Pd–N 2.016(6) Å]. By potentiometry, pK_a values of 2.58 (CO_2H), 8.63 (HisεNH, 'pyrrole nitrogen') and 11.50 (co-ordinated NH_2) for **1** and 11.30 (HisεNH) for **2** were determined and confirmed by ^{1}H NMR spectroscopy.

Our interest in peptide complexes of gold(III) arises from the recent proposal that it may be involved in the immunological side-effects of anti-arthritic gold(I) drugs.[1,2] For example, it has been reported that chronic treatment of mice with Au^I drugs results in the production of T cells (white blood cells) that are stimulated not by gold(I) but by gold(III).[1] These T cells recognize peptides, and Au^{III} peptides could be involved in these immunological reactions. Oxidation of gold(I) to gold(III) may be mediated by the enzyme myeloperoxidase *via* formation of hypochlorite.[3]

While the reduction of Au^{III} by cysteine and methionine side-chains of amino acids and peptides is well established,[4] only two crystal structures of Au^{III} peptide complexes have previously been described:[5] those of the dipeptide glycyl-L-histidine (Gly-L-His), $[Au(Gly\text{-}L\text{-}His\text{-}H_{-1})Cl]Cl\cdot 3H_2O$ and $[Au(Gly\text{-}L\text{-}His\text{-}H_{-2})]_4\cdot 10H_2O$. Several crystal structures of peptide complexes of other square-planar metal ions have been reported. Peptide–copper(II) complexes are the most extensively studied and, among others, crystal structures of di-, tetra- and pentaglycine with Cu^{II} have been reported[6] as well as a crystal structure of Cu^{II} and glycylglycyl-L-histidine-*N*-methyl amide.[7] Nickel(II)–peptide complexes have also been widely studied, and reported crystal structures include the square-planar complex of Ni^{II} with tetraglycine.[8] The only crystal structure of a copper(III) peptide is that of tri-α-aminoisobutyric acid,[9] a derivative of trialanine with two methyl groups attached to the α-carbon. Palladium(II)–peptide complexes have been widely studied and the available crystal structures are for complexes of glycyl-L-tyrosine and cytidine,[10] glycyl-DL-methionine[11] and glycyl-L-histidine.[12] The only peptide crystal structures of platinum(II) are of glycyl-L-methionine[13] and diglycine[14] complexes. A particular feature of these metal ions is their ability to deprotonate peptide bond NH groups, which in free peptides have pK_a values of *ca.* 15, at low pH values (2–8).[15]

† *Present address*: Department of Chemistry, University of Edinburgh, King's Buildings, West Mains Road, Edinburgh, UK EH9 3JJ.

The aromatic nature of the imidazole ring has to be considered when examining the ability of the His ring to act as a ligand for transition metals. Only one of the nitrogen atoms of the ring, δN (the 'pyridine nitrogen'), possesses a lone pair of electrons. The electrons of the εN (the 'pyrrole nitrogen') take part in the aromatic ring system, *i.e.* they are delocalized throughout the system and therefore binding of a proton or a metal ion is expected to be very unfavourable at this site. The pK_a values reflect this prediction. At low pH, δN is protonated (the distinction between the two nitrogen atoms is lost) and deprotonates with a pK_a of 7.1 (for imidazole). The εN of imidazole undergoes an additional deprotonation with reported pK_a values of 14.2–14.6.[16] The acidity of εN (the 'pyrrole nitrogen') increases upon complexation of a metal ion at δN (the 'pyridine nitrogen'), a process referred to as 'across-the-ring-ionization'.[17] For example, in the copper(II) complex of Gly-Gly-L-His, the εNH group deprotonates with a pK_a value of about 10.7,[18] and for cobalt(II) complexed to L-histidine or imidazole, approximate pK_a values of 12.5 have been measured for the deprotonation of the 'pyrrole nitrogen'.[19] In contrast, no deprotonation below pH 12 was measurable for a complex of L-histidine and nickel(II).[20] Even lower pK_a values have been reported when the εN-bound proton is replaced by a second metal ion, *e.g.* pK_a values of around 9.6 have been measured in complexes of copper(II), nickel(II) and palladium(II) with Gly-L-His, and a tetrameric structure with a bridging imidazole has been proposed to form at high pH. A similar tetrameric imidazole–gold(III)-bridged complex of Gly-L-His was crystallized from a solution at pH 6–7.[5] The ability of Au^{III} to lower the pK_a of HisεNH, when complexed to HisδN, has not yet been investigated.

In this work we have studied the complexation of Au^{III} to the tripeptide Gly-Gly-L-His (GGH, L), at various pH values, by ^{1}H NMR spectroscopy and investigated deprotonation by ^{1}H NMR and potentiometry. For comparison, analogous reactions of Pd^{II} have also been studied. The peptide GGH has been used as a model for the N-terminal square-planar copper(II) and

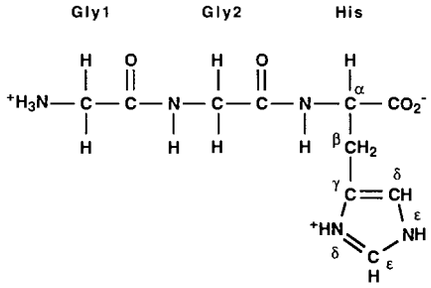

L (Gly-Gly-L-His)

nickel(II) binding site of serum albumin.[21] This is the first report of crystal structures of Au^{III} and Pd^{II} tripeptide complexes.

Experimental

Materials

The peptide Gly-Gly-L-His (acetate salt, *ca.* 0.5–1.0 acetate mol^{-1}) and $NiSO_4 \cdot 6H_2O$ were purchased from Sigma, and $Na[AuCl_4] \cdot nH_2O$ ($n \approx 2$) as well as $K_2[PdCl_4]$ from Johnson Matthey plc.

NMR Spectroscopy

Proton NMR spectra were recorded on JEOL GSX270 and GSX500 spectrometers at 270 and 500 MHz respectively, in 5 mm tubes, using dioxane as internal reference (δ 3.764 relative to sodium 3-(trimethylsilyl)tetradeuteriopropionate at 310 K). Typical pulsing conditions: spectral width 3.2–5.0 KHz (6.0–9.0 KHz at 500 MHz), pulse width 45°, relaxation delay 2.2 s, 16 or 32 K data points, 128 transients. Spectra were processed using exponential functions equivalent to a line-broadening of 0.4 Hz. Coupling constants were determined from spectra that were zero-filled once and processed using exponential functions equivalent to a line-broadening of the same value as the respective resolution. The two-dimensional total correlation spectrum (TOCSY) was obtained at 500 MHz with a mixing time of 70 ms, 32 scans, 256 increments of f_1, relaxation delay 2.5 s and 2 K points (f_2). It was zero-filled to 4 × 1 K and processed using a shifted squared sinebell as window function.

Typically, to follow the time course of the reaction, 0.7 ml of a 10 mM solution of Gly-Gly-L-His in D_2O was prepared and the pH* adjusted to 2 with DNO_3. A similar sample served as a control. The salt $Na[AuCl_4]$ was then added as a 20 μl aliquot of a fresh stock solution in D_2O and the pH* remeasured. Signals for the HisεCH proton for all reaction products were well resolved and these were therefore integrated relative to the reference peak of dioxane to obtain relative percentages of the different species in solution during the course of the reaction. A buffered reaction at pH* 2 was carried out in 0.33 M deuteriated phosphoric acid buffer. Reactions at pH* 4 and 5 were carried out in 0.1 M deuteriated acetate buffer. Reactions at pH* 7 were carried out in 0.1 M sodium phosphate buffer in D_2O.

The pH titrations of crystalline $[Au^{III}(Gly\text{-}Gly\text{-}L\text{-}His\text{-}H_{-2})]Cl \cdot H_2O$ **1** and $[Pd^{II}(Gly\text{-}Gly\text{-}L\text{-}His\text{-}H_{-2})] \cdot 1.5H_2O$ **2** were carried out on 10 mM solutions of the respective crystals, titrating them with NaOD and measuring ^1H NMR spectra at intervals of about 0.5 pH units. Because the palladium(II) complex with GGH is insoluble in water at low pH values, the pH of the solution was first adjusted to about pH* 7 with NaOD to dissolve the crystals and ^1H NMR spectra of the compound were obtained in the range pH* 7–13 only. Measurements of pH were made using an Aldrich micro combination electrode and Corning 240 meter, calibrated with Aldrich buffer solutions. Readings of the pH meter for D_2O solutions were not corrected for deuterium isotope effects and are designated as pH* values. The resulting pH titration curves were fitted to a modified form of the Hill equation[22] using the program KALEIDAGRAPH on an Apple Macintosh computer.[23]

The nickel(II) complex of GGH forms above pH 6.5[24] and is essentially 100% abundant above pH 8.[25] Because the complex is prone to slow air-oxidation,[26] solutions of 10 mM GGH in D_2O were made up and addition of 0.9 mol equivalent of nickel sulfate, followed by adjustment of the pH* to the desired value with NaOD, was carried out immediately before the NMR measurements.

Potentiometry

Protonation constants of the complexes $[Au^{III}(Gly\text{-}Gly\text{-}L\text{-}His\text{-}H_{-2})]Cl$ and $[Pd^{II}(Gly\text{-}Gly\text{-}L\text{-}His\text{-}H_{-2})]$ were also determined by pH-metric measurements. Solutions of the complexes (4 mM) were titrated with carbonate-free potassium hydroxide in the range pH 2–12 for gold(III), and 7–12 for palladium(II) complexes. All pH-metric measurements were made at 298 K at a constant ionic strength of 0.2 M (KCl). Argon was bubbled through the samples to ensure the absence of oxygen and carbon dioxide and for stirring the solutions. Measurements were performed with a Radiometer PHM84 pH-meter equipped with a GK2421C combined electrode and an ABU 13 automatic burette containing the potassium hydroxide. The pH-readings were converted to $[H^+]$ ion concentration[27] and the protonation constants were calculated by means of a general computational program PSEQUAD.[28]

Crystallization of complex 1

The peptide Gly-Gly-L-His (162.9 mg, 0.5 mmol) was dissolved in water (10 ml) and the pH of the solution adjusted to 2.4 by addition of 1 M HNO_3. To this was added $Na[AuCl_4]$ (199.5 mg, 0.5 mmol) dissolved in water (0.15 ml) to give a final concentration of the reactants of 46 mM, pH 2.4. This was left in the dark in a water-bath at 310 K for at least 3 d. Any colloidal gold formed was removed by filtration and the volume of the yellow solution (pH typically about 1) was reduced to 4 ml by slow evaporation at ambient temperature. Pale yellow crystals of $[Au^{III}(Gly\text{-}Gly\text{-}L\text{-}His\text{-}H_{-2})]Cl \cdot H_2O$ formed at 277 K several days after the addition of twice the volume of acetone. These were filtered off, washed twice with cold acetone, and dried in the dark at ambient temperature. Yield *ca.* 30% (Found: C, 23.45; H, 2.42; N, 13.14. $C_{10}H_{13}AuClN_5O_4 \cdot H_2O$ requires C, 23.20; H, 2.92; N, 13.53%).

Crystallization of complex 2

The peptide Gly-Gly-L-His (32.6 mg, 0.1 mmol) was dissolved in water (10 ml) and the pH of the solution adjusted to 2.4 by addition of 1 M HNO_3. To this was added $K_2[PdCl_4]$ (33.1 mg, 0.1 mmol) dissolved in water (0.5 ml) to give a final concentration of the reactants of 10 mM. The pH of the light brown solution was 1.6. The solution was left standing at ambient temperature in the dark. After 15 h, copious small light brown crystals of $[Pd^{II}(Gly\text{-}Gly\text{-}L\text{-}His\text{-}H_{-2})] \cdot 1.5H_2O$ appeared which were filtered off, washed with water and dried *in vacuo*. Yield *ca.* 76% (Found: C, 30.35; H, 3.74; N, 17.23. $C_{10}H_{13}N_5O_4Pd \cdot 1.5H_2O$ requires C, 29.98; H, 3.65; N, 17.48%).

Crystal structure determinations for complexes 1 and 2

Crystal data. *Complex* **1**. $C_{10}H_{13}AuClN_5O_4 \cdot H_2O$, $M = 517.68$, orthorhombic, space group $P2_12_12_1$, $a = 9.437(2)$, $b = 10.1389(8)$, $c = 15.812(1)$ Å, $U = 1512.9(4)$ $Å^3$ [by least-squares refinement of 25 intense reflections, with $\theta > 40°$, $\lambda = 1.541\,78$ Å, $T = 291(2)$ K], $Z = 4$, $D_c = 2.273$ Mg m^{-3}, $F(000) = 984$, yellow stable crystal, needle 0.3 × 0.3 × 0.4 mm, μ(Cu-Kα) = 20.128 mm^{-1}.

Complex **2**. $C_{10}H_{13}N_5O_4Pd \cdot 1.5H_2O$, $M = 400.68$, orthorhombic, space group $C222_1$, $a = 19.024(2)$, $b = 14.640(1)$, $c = 9.824(1)$ Å, $U = 2736.1(4)$ $Å^3$ [by least-squares refinement of

25 intense reflections, with $\theta > 40°$, $\lambda = 1.541\,80$ Å, $T = 291(2)$ K], $Z = 8$, $D_c = 1.945$ Mg m^{-3}, $F(000) = 1608$, white stable crystal, needle 0.1 × 0.2 × 0.5 mm, μ(Cu-Kα) = 11.277 mm^{-1}.

Data collection and processing. *Complex* **1**. CAD4 diffractometer, ω–2θ mode, graphite-monochromated Cu-Kα radiation, $5.18 < \theta < 71.84°$, $0 < h < 11$, $-12 < k < 0$, $0 < l < 19$, 1717 reflections of which 1694 with $I > 2\sigma(I)$. Absorption corrections with DIFABS[29] made at an intermediate stage of the analysis. Minimum, maximum, average absorption corrections were 0.173, 1.326, 0.650.

Complex **2**. CAD4 diffractometer, ω–2θ mode, graphite-monochromated Cu-Kα radiation, $3.81 < \theta < 72.01°$, $-23 < h < 0$, $-18 < k < 0$, $-10 < l < 12$, 2808 reflections (2645 independent, $R_{int} = 0.051$) of which 2579 with $I > 2\sigma(I)$. Absorption corrections with DIFABS made at an intermediate stage of the analysis. Minimum, maximum, average absorption corrections were 0.339, 1.236, 0.601.

Structure analysis and refinement. *Complex* **1**. Heavy atom method using SHELXS 86[30] and SHELXL 93;[31] subsequent refinement by full-matrix least squares on $|F^2|$, anisotropic displacement parameters for non-H atoms, isotropic for H-atoms in geometrically fixed, riding mode; $w = 1/[\sigma^2(F_o^2) + (0.2276P)^2 + 1.4584P]$ where $P = (F_o^2 + 2F_c^2)/3$ gave satisfactory weights with $S = 1.069$ on F^2. Final R factors were $R1 = 0.0387$ (on F), $wR2 = 0.1015$ (on F^2) for 1717 reflections and 210 parameters. An extinction parameter refined to a value of 0.022(2). The absolute configuration of the histidine was confirmed to be L through use of anomalous X-ray scattering factors and determination of the Flack parameter[32] which refined to a value of −0.03(3) compared to a theoretical value of 0.0. The final difference electron density had values between 1.758 and −0.976 e Å^{-3}. Least-squares refinement converged with a mean Δ/error of 0.022 (maximum 0.133 for the extinction parameter).

Complex **2**. Heavy atom method using SHELXS 86 and SHELXL 93; subsequent refinement by full-matrix least squares on $|F^2|$, anisotropic displacement parameters for non-H atoms, fixed isotropic for H-atoms in geometrically fixed, riding mode. Hydrogen atoms on the carboxyl O(31) and on the waters were modelled to form acceptable H bonds and subsequently fixed; $w = 1/[\sigma^2(F_o^2) + (0.0663P)^2 + 17.4096P]$ where $P = (F_o^2 + 2F_c^2)/3$ gave satisfactory weights with $S = 1.172$ on F^2. Final R factors were $R1 = 0.0465$ (on F), $wR2 = 0.1366$ (on F^2) for 2645 reflections and 197 parameters. An extinction parameter refined to a value of 0.000 03(1). The absolute configuration of the histidine was confirmed to be L through use of anomalous X-ray scattering factors and determination of the Flack parameter which refined to a value of 0.03(2) compared to a theoretical value of 0.0. The final difference electron density had values between 1.758 and −0.976 e Å^{-3}. Least-squares refinement converged with a mean Δ/error of 0.022 (maximum 0.133 for the extinction parameter). Drawings were produced by the program SNOOPI.[33]

Atomic coordinates, thermal parameters, and bond lengths and angles have been deposited at the Cambridge Crystallographic Data Centre (CCDC). See Instructions for Authors, *J. Chem. Soc., Dalton Trans.*, 1997, Issue 1. Any request to the CCDC for this material should quote the full literature citation and the reference number 186/558.

Results

Crystal structure of complex 1

The crystal structure of [Au^{III}(Gly-Gly-L-His-H$_{-2}$)]Cl·H$_2$O (**1**, Fig. 1) shows Au^{III} in a square-planar co-ordination environment bound to the terminal amino group, two deprotonated peptide amide nitrogens and δN of the histidine side-chain. The carboxyl group is protonated and H-bonded to a water molecule [O(w)]. Selected bond lengths and angles are shown in Tables 1–3. Two five-membered rings are formed, encompassing the amino–terminal amino group and the two deprotonated peptide bonds, and one six-membered ring which includes the histidine side-chain. The longest Au–N bond is between gold(III) and the terminal amino nitrogen [N(0), 2.049(10) Å]. The bonds to the deprotonated amide nitrogens of the peptide bonds are shorter [Au–N(1) 1.941(9) Å, Au–N(2) 2.006(10) Å], the shortest being Au–N(1) which is part of the two five-membered rings. The smallest angles in the square-planar geometry around the metal are found in the two five-membered rings [N(1)–Au–N(0) 82.8(4)° and N(2)–Au–N(1) 83.5(4)°]. The angle formed at Au by the six-membered ring is 93.3(4)° [N(34)–Au–N(2)]. The largest angle of 100.4(4)° is situated on the open side of the chelate ring. The bond lengths in the peptide part of **1** correspond to bond lengths found in crystal structures of uncomplexed amino acids and peptides[34] within the experimental uncertainty of three times the standard deviation.

Table 1 Selected bond lengths (Å) for complexes **1** and **2**

	1 (M = Au)	**2** (M = Pd)
M–N(34)	2.038(9)	2.016(6)
M–N(2)	2.006(10)	1.983(6)
M–N(1)	1.941(9)	1.943(7)
M–N(0)	2.049(10)	2.058(7)
C(11)–O(11)	1.22(2)	1.259(11)
C(11)–N(1)	1.33(2)	1.306(11)
C(21)–O(21)	1.19(2)	1.258(10)
C(21)–N(2)	1.35(2)	1.323(10)

Table 2 Selected bond angles (°) for complexes **1** and **2**

	1 (M = Au)	**2** (M = Pd)
N(34)–M–N(2)	93.3(4)	95.0(3)
N(2)–M–N(1)	83.5(4)	82.1(3)
N(1)–M–N(0)	82.8(4)	83.4(3)
N(0)–M–N(34)	100.4(4)	99.6(3)

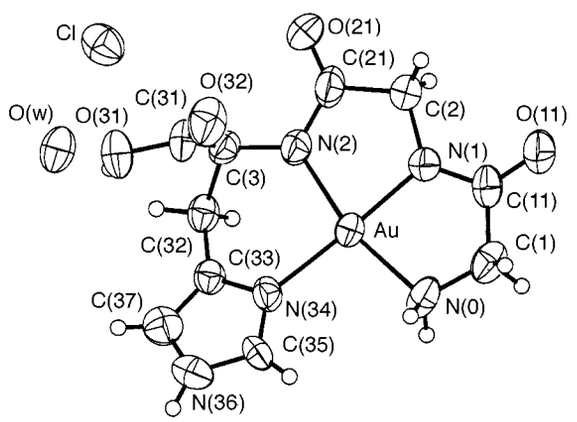

Fig. 1 Crystal structure of [Au^{III}(Gly-Gly-L-His-H$_{-2}$)]Cl·H$_2$O **1**, and numbering scheme. The water molecule O(w) is H bonded to the carboxyl group. Thermal ellipsoids are shown at the 50% probability level

Crystal structure of complex 2

The crystal structure of [Pd^{II}(Gly-Gly-L-His-H$_{-2}$)]·1.5H$_2$O (**2**, Fig. 2) shows that the complex is also square-planar with Pd^{II} bound to the terminal amino group, two deprotonated peptide amide nitrogens and δN of His. Selected bond lengths and angles are shown in Tables 1, 2 and 4. Analogous to the gold(III) complex, the longest Pd–N bond is the one between palladium(II) and the terminal amino nitrogen [N(0), 2.058(7) Å]. The bonds to the deprotonated amide nitrogens of the peptide

Table 3 Intra- and inter-molecular hydrogen bonding and close contacts to H_2O and Cl for complex **1**

Acceptor atom (A)	Hydrogen (H)	Donor atom (D)	Distance (D ··· A)/Å
$O(1^{I})$ water	$H(31^{I})$	$O(31^{I})$	2.523
O(11)	$H(12^{II})$	$O(1^{II})$ water	2.654
$O(32^{III})$	H(0B)	N(0)	2.850
O(21)	$H(36^{IV})$	$N(36^{IV})$	2.863
$Cl(6^{I})$	$H(11^{I})$	$O(1^{I})$ water	3.077
$O(31^{V})$	$H(0A^{I})$	$N(0^{I})$	3.261

Symmetry operations: I, x, y, z; II, $\frac{1}{2}+x, \frac{1}{2}-y, -z$; III, $-\frac{1}{2}+x, \frac{1}{2}-y, -z$; IV, $1+x, y, z$; V, $\frac{1}{2}-x, -y, \frac{1}{2}+z$.

Table 4 Intra- and inter-molecular hydrogen bonding and close contacts to H_2O for complex **2**

Acceptor atom (A)	Hydrogen (H)	Donor atom (D)	Distance (D ··· A)/Å
$O(31^{I})$	$H(31B^{II})$*	$O(31^{II})$	2.938
$O(1^{I})$ water	$H(0B^{I})$	$N(0^{I})$	2.855
$O(21^{I})$	$H(36^{III})$	$N(36^{III})$	2.752
$O(32^{I})$	$H(11^{IV})$	$O(1^{IV})$ water	2.947
$O(21^{I})$	$H(2^{I})$	$O(2^{I})$ water	3.096
$O(21^{I})$	$H(0A^{V})$	$N(0^{V})$	3.183
$O(11^{I})$	$H(31A^{V})$	$O(31^{V})$	3.385

* The H position on O(31) is shared by H(31A) and H(31B), the latter with coordinates: 0.515, 0.780, 0.800. Symmetry operations: I, x, y, z; II, $1-x, y, \frac{1}{2}-z$; III, $x, y, 1+z$; IV, $\frac{3}{2}-x, -\frac{1}{2}+y, \frac{3}{2}-z$; V, $\frac{3}{2}-x, \frac{3}{2}-y, \frac{1}{2}+z$.

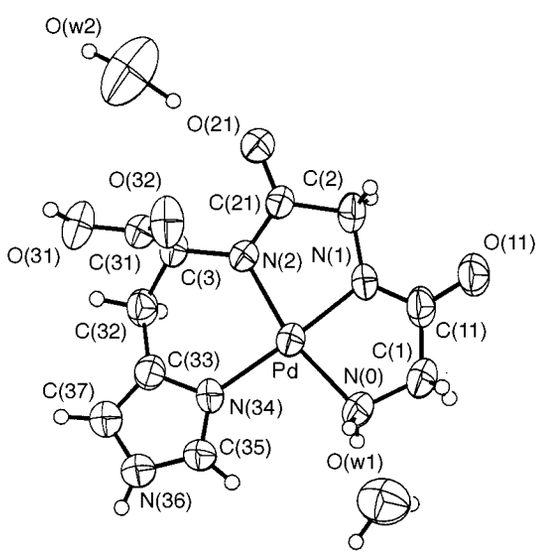

Fig. 2 Crystal structure of $[Pd^{II}(Gly\text{-}Gly\text{-}L\text{-}His\text{-}H_{-2})]\cdot 1.5H_2O$ **2**, and numbering scheme. Thermal ellipsoids are shown at the 50% probability level

bonds are shorter [Pd–N(1) 1.943(7) Å, Pd–N(2) 1.983(6) Å], the shortest again being the metal–N(1) bond which is part of two five-membered rings. The smallest angles in the square-planar geometry around the metal are 83.4(3)° [N(1)–Pd–N(0)] and 82.1(3)° [N(2)–Pd–N(1)] in the two five-membered rings. The angle in the six-membered ring system is 95.0(3)° [N(34)–Pd–N(2)] and the largest angle of 99.6(3)° is again situated on the open side of the chelate ring. The bond lengths in the peptide part of **2** correspond to bond lengths found in crystal structures of uncomplexed amino acids and peptides [34] within the experimental uncertainty of twice the standard deviation.

Planarity of complexes 1 and 2

The deviations from the co-ordination square-plane are smaller for the gold(III) complex than for the palladium(II) complex. In the gold(III) complex, the deviations from the least-squares plane through Au, N(0), N(1), N(2) and N(34) calculated from the equation $0.681(36)x + 7.916(22)y - 9.815(44)z = 0.182(11)$ are very small: 0.003(6) Å for N(0), −0.006(7) Å for N(1), 0.004(6) Å for N(2), −0.005(5) Å for N(34) and 0.004(4) Å for Au. The root-mean-square deviation of the atoms from the fitted plane is 0.005 Å. The least-squares plane fitted through the five atoms of the imidazole ring [C(33), N(34), C(35), N(36) and C(37)] with the equation $-2.246(56)x - 6.537(50)y + 11.485(68)z = 0.153(5)$ forms an angle of 20.44(60)° with the above described plane through Au and the four donor nitrogens.

In the palladium(II) complex the deviations from the least-squares plane through Pd, N(0), N(1), N(2) and N(34) calculated from the equation $0.866(54)x + 14.614(3)y + 0.377(27)z = 13.707(45)$ were found to be −0.050(5) Å for N(0), 0.045(6) Å for N(1), −0.054(5) Å for N(2), 0.030(4) Å for N(34) and 0.029(3) Å for Pd. The root-mean-square deviation of the atoms from the fitted plane is 0.043 Å. The atoms N(0) and N(2) lie below the least-squares plane while N(1), N(34) and Pd are above the plane. The least-squares plane fitted through the five atoms of the imidazole ring [C(33), N(34), C(35), N(36) and C(37)] with the equation $3.323(86)x + 14.281(16)y - 1.317(47)z = 14.037(59)$ forms an angle of 12.44(16)° with the above described plane through Pd and the four donor nitrogens.

Reaction of GGH with $[AuCl_4]^-$

The aromatic and aliphatic regions of ^{1}H NMR spectra recorded during the reaction of 8.8 mM GGH with 1 mol equivalent of $Na[AuCl_4]$ in D_2O at an initial pH* value of 2.0 are shown in Fig. 3. The reaction is relatively slow, with a half-life of 9.3 h at 310 K. After 62 h, the pH* of the reaction mixture had dropped to 1.2. During the reaction some colloidal gold was seen, and an intermediate **3** peaked in concentration after *ca.* 2 h and was present for *ca.* 23 h. A minor product **4** was first seen after *ca.* 3 h and was present in a decreasingly small amount until the end of the monitoring period (*ca.* 62 h). The amount of **4** increased considerably in reaction mixtures of the same pH* that contained more than 1 mol equivalent of $Na[AuCl_4]$ (data not shown). In those spectra, it could be seen that the chemical shifts of $Gly1CH_2$, $Gly2CH_2$ and $His\beta CH_2$ of **4** were close to those of **1**, and that **4** showed the same inequivalent $Gly2CH_2$ methylene protons and large shift difference of the $His\beta CH_2$ protons. The typical small $^4J(\beta'CH\text{–}\delta CH)$ coupling could not be seen for **4** because of overlap with the signals for the major product **1**. After *ca.* 5 h, small peaks for another minor product **5** were detectable in the HisεCH (overlapped with the resonance for the free ligand) and the glycine CH_2 regions (Fig. 3). Some colloidal gold was seen at the end of the reaction. It was shown in an independent experiment that the reduction of gold(III) is not due to the acetate which is present in the commercially available GGH preparations. Product **5** accounted for less than 1% of the products in a 1:1 GGH:$Na[AuCl_4]$ reaction carried out in phosphoric acid buffer, pH* 2, where the major product was **1** (97%) and the minor product **4** (2 to 3%). The major final product had the same ^{1}H NMR spectrum as crystalline **1**, Tables 5 and 6. The HisεCH resonances of intermediates and products showed upfield shifts compared to the free ligand $\Delta\delta$ 0.23 ppm for **3**, 0.32 ppm for **1** and the largest shift of 0.54 ppm for **4**. For the HisδCH proton, only the intermediate **3** showed a significant (upfield) shift compared to the free ligand (0.035 ppm).

The most notable feature in the spectrum of the major product **1**, Fig. 4, is the observable $^4J(\beta'CH\text{–}\delta CH)$ coupling which was not seen for GGH itself. This characteristic coupling was also seen for complexes of GGH with palladium(II) and nickel(II). Another feature of the ^{1}H NMR spectrum typical of the chelate is the magnetic non-equivalence of the methylene protons of Gly2 and the larger chemical shift difference

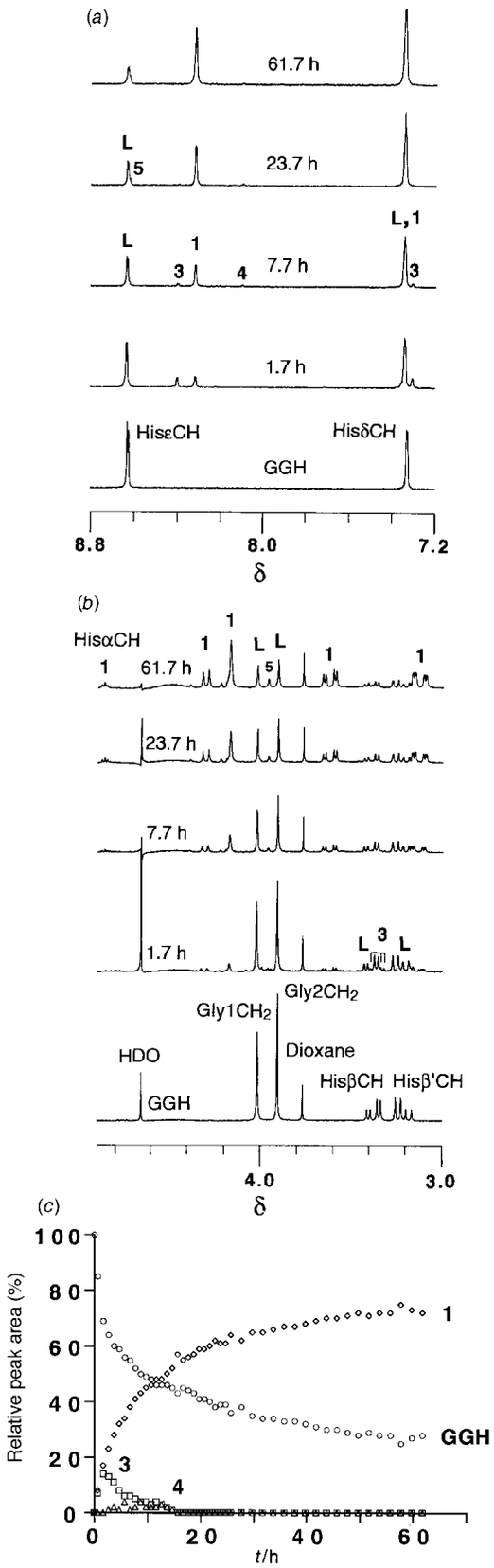

Fig. 3 The 270 MHz ^{1}H NMR spectra of Gly-Gly-L-His (L, 8.8 mM) in D_2O before and at various times after the addition of 1 mol equivalent of Na[$AuCl_4$], 310 K, initially at pH* 2.0, showing peaks for Gly-Gly-L-His, the product [Au^{III}(Gly-Gly-L-His-H_{-2})]$^+$ **1**, an intermediate **3** and a minor product **4**. (*a*) Aromatic region, (*b*) aliphatic region, (*c*) plot of relative peak areas of HisεCH peaks (compared to reference dioxane and as percentage of the sum of peak areas of all species for this proton) *versus* reaction time

of the HisβCH_2 protons than in the uncomplexed ligand. These features are also seen in the complexes of GGH with

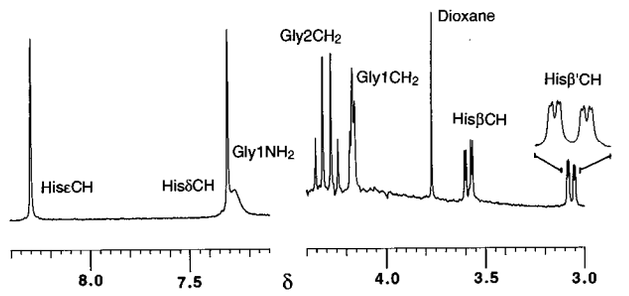

Fig. 4 The ^{1}H NMR spectrum of **1** in 90% H_2O–10% D_2O, pH 2.67; the expansion of the Hisβ′CH multiplet shows the ^4J coupling. The observation of this coupling is characteristic for square-planar complexes of metals with GGH and is not seen for the free ligand. In $(CD_3)_2SO$ the Gly1NH_2 peak is resolved into two separate resonances. The signal for the HisαCH proton (not shown) is affected by the presaturation of the nearby water resonance

palladium(II) and nickel(II). The ^{1}H NMR spectrum for complex **1** in 90% H_2O–10% D_2O at low pH, Fig. 4, shows an additional peak for the NH_2 protons of the terminal amino group which cannot be observed for the peptide itself due to the fast exchange,[35] showing that their exchange rate is lowered by complexation. No peaks for the NH protons of the two peptide bonds, which are observable in GGH at low pH, were observable for **1**, which confirms the metal-induced deprotonation of the amide bonds.

pH Dependence of reaction of GGH with [$AuCl_4$]$^-$

The square-planar product **1** was still formed when the starting pH of the reaction was as low as 1.5; however, the reaction was considerably slower. On the contrary, an increase in the starting pH value to 2.5 led to the main product being formed slightly faster. The reaction was also faster when the reaction mixture was buffered at pH* 2 with phosphoric acid buffer. When the reaction was carried out in acetate buffer at pH* 4 and 5, there was partial precipitation of a GGH-containing material, and the only observable product detected by ^{1}H NMR was **1**; no intermediate was seen. When [$AuCl_4$]$^-$ was titrated into a GGH solution in 0.1 M sodium phosphate buffer at pH* 7 (0.25, 0.5, 0.75, 1.0 mol equivalents), the only ^{1}H NMR peaks seen were those for unreacted L, such that at a 1:1 mol ratio of Au:GGH no peaks at all were observed, except the peaks for acetate and the secondary reference dioxane (data not shown), and some precipitate was formed.

Reaction of GGH with [$PdCl_4$]$^{2-}$

The anion [$PdCl_4$]$^{2-}$ reacted rapidly with GGH (1:1 mol ratio) at low pH* values, 310 K. When a fresh solution of K_2[$PdCl_4$] was added to a solution of GGH in D_2O, pH* 2.0 (final concentration of both reactants 8.9 mM), the pH* dropped immediately to 1.6. After 40 min, only about 4% of the original HisεCH peak intensity was detectable for GGH and resonances for one product were seen which showed the typical upfield shift of the Hisβ′CH proton for square-planar metal complexes of GGH. All resonances were severely broadened. After 17 h, no uncomplexed ligand was detectable. The final pH* of the reaction mixture after 60 h was 1.1. Crystals of **2** formed during the course of the reaction. These crystals redissolved at pH* 7. Chemical shifts and coupling constants for **2** are listed in Tables 5 and 6. The same complex also formed at neutral pH. In a $(CD_3)_2SO$ solution of **2**, peaks for the terminal NH_2 protons, CO_2H and εNH of His were also seen. The assignments of the very low field peaks for COOH and HisεNH were made on the basis of a two-dimensional TOCSY experiment which showed connectivities between HisεNH, HisδCH and HisεCH resonances. Product **2** was stable in D_2O or $(CD_3)_2SO$ for at least 2 weeks.

Table 5 Proton NMR chemical shifts δ of GGH (pH* 7.0), **1** (pH* 7.0), **2** (pH* 7.3) and $[Ni^{II}(Gly\text{-}Gly\text{-}L\text{-}His\text{-}H_{-2}]^-$ (NiGGH) (pH* 7.0) in D_2O, 270 MHz; co-ordination shifts Δδ ($\delta_{MGGH} - \delta_{GGH}$) are shown in parentheses

Proton	GGH	**1**	**2**	NiGGH
$Gly1CH_2$	3.864	4.156 (+0.292)	3.635 (−0.229)	3.198 (−0.666)
Gly2CH	3.983	4.314 (+0.331)	3.914[a] (−0.069)	3.465[b] (−0.518)
Gly2CH′	3.983	4.254 (+0.271)	3.895[a] (−0.088)	3.443[b] (−0.540)
HisαCH	4.494[c]	4.522 (+0.028)	4.307 (−0.187)	3.968 (−0.526)
HisβCH	3.213[c]	3.510 (+0.297)	3.263 (+0.050)	3.095 (−0.118)
Hisβ′CH	3.061[c]	2.984 (−0.077)	2.753 (−0.308)	2.790 (−0.271)
HisδCH	7.116	7.254 (+0.138)	6.972 (−0.144)	6.877 (−0.239)
HisεCH	8.203	8.265 (+0.062)	7.599 (−0.604)	7.313 (−0.890)
HisεNH	*d*	*d*	12.591[e]	*d*
$HisCO_2H$	*d*	*d*	12.010[e]	*d*
$Gly1NH_3^+$	*d*	7.277[f]	4.598[e]	*d*
($Gly1NH_2$)			4.718[e]	

[a] 500 MHz, **2** in 90% H_2O–10% D_2O, pH 6.9. [b] 500 MHz, NiGGH in 90% H_2O–10% D_2O, pH 7.3. [c] Mean chemical shift value of splitting pattern. [d] Not determined. [e] Complex **2** in $(CD_3)_2SO$. [f] Complex **1** in 90% H_2O–10% D_2O, pH 2.7.

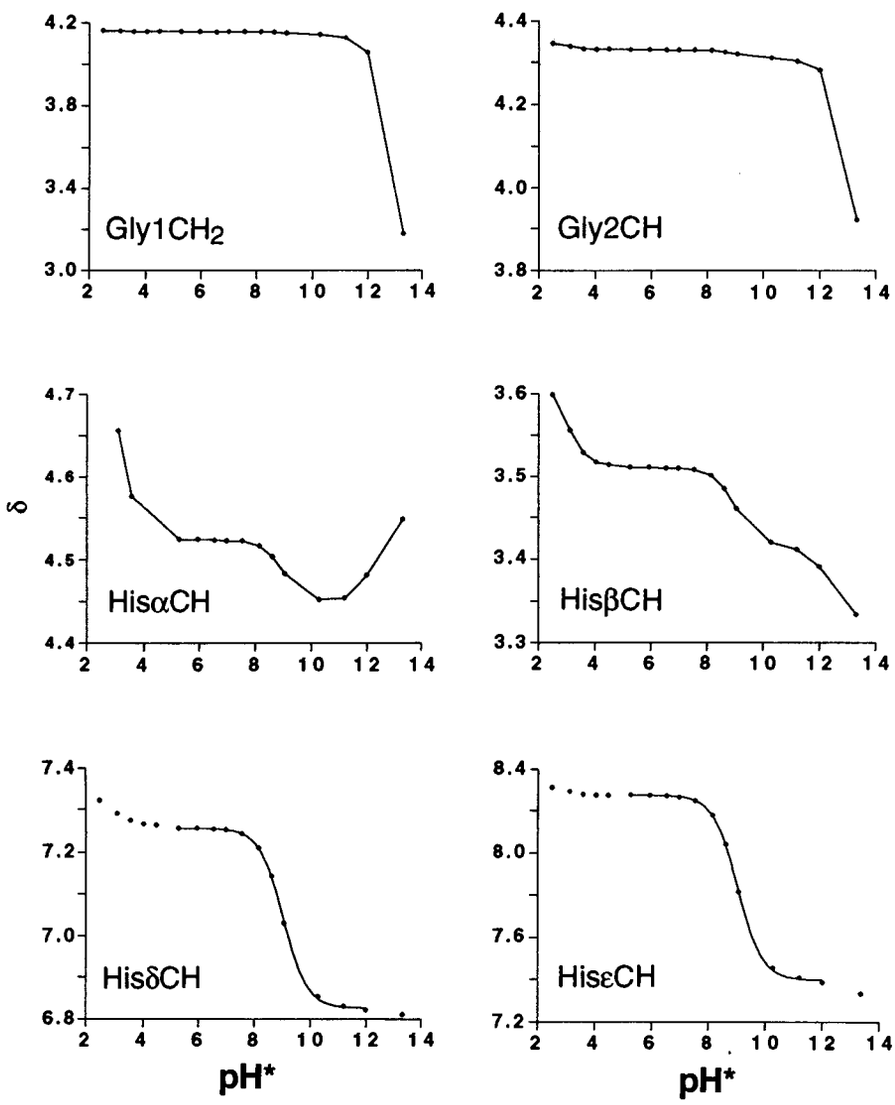

Fig. 5 Plots of ^1H NMR chemical shifts of $[Au^{III}(Gly\text{-}Gly\text{-}L\text{-}His\text{-}H_{-2})]^+$ **1** *versus* pH*. The curves (solid line) shown for HisδCH and HisεCH are computer best-fits corresponding to a pK_a value of 9.04 ± 0.01 (HisεNH). The large shifts for $Gly1CH_2$ and $Gly2CH_2$ correspond to deprotonation of the terminal amino group. Below pH* 4 the His CO_2H group titrates. The HisαCH is affected by all three deprotonation reactions

Deprotonation of the 'pyrrole nitrogen' (HisεNH)

The pH* dependences of the ^1H NMR spectra of the crystalline complexes **1** and **2** were investigated. Plots of the chemical shifts (δ) of all resonances observable in D_2O *versus* pH* are shown in Fig. 5 for $[Au^{III}(Gly\text{-}Gly\text{-}L\text{-}His\text{-}H_{-2})]Cl$ **1**. Below pH* 5, changes in shift of all resonances except $Gly1CH_2$ were observed, consistent with the deprotonation of the terminal His carboxylate group. At alkaline pH*, large shifts of HisδCH and HisεCH were observed and were fitted to a pK_a value of 9.04 ± 0.01. At very high pH* (>11) large shifts of peaks for $Gly1CH_2$ and $Gly2CH_2$ were seen. The HisαCH resonance shows shifts due to the presence of three different titrating groups. It can be seen from this resonance that two separate

Table 6 Proton NMR coupling constants J (Hz ± 0.2) in GGH (in 90% H_2O–10% D_2O, pH 3.1), **1** (in D_2O, pH* 3.1), **2** (in D_2O, pH* 7.3) and $[Ni^{II}(Gly\text{-}Gly\text{-}L\text{-}His\text{-}H_{-2})]^-$ (NiGGH) (in D_2O, pH* 8.1)

	GGH	**1**	**2**	NiGGH
^3J(Gly1NH_2–Gly1CH_2)	5.2[a]	5.7[b]	6.2[c]	*d*
^3J(Gly2NH–Gly2CH_2)	5.9	n.a.	n.a.	n.a.
^2J(Gly2CH–Gly2CH′)	17.2	17.8	18.9	18.4
^3J(HisNH–HisαCH)	8.1	n.a.	n.a.	n.a.
^3J(HisαCH–HisβCH)	5.1	3.9	3.9	3.3
^3J(HisαCH–Hisβ′CH)	8.3	3.9	3.9	4.3
^2J(HisβCH–Hisβ′CH)	15.4	15.8	15.2	15.0
^4J(Hisβ′CH–HisδCH)		1.4	1.2	1.4
^4J(HisδCH–HisεCH)	1.3	1.0	1.2	1.2

n.a. not applicable. [a] ±0.31, GGH, pH = 1.6, freeze-dried and redissolved in $(CD_3)_2SO$. [b] **1** in 90% H_2O–10% D_2O, pH 2.7. [c] **2** in 90% H_2O–10% D_2O, pH 6.9. [d] Not determined.

titrating groups are responsible for the chemical shifts at alkaline pH* values as the pK_a value of 9.04 leads to upfield shifts, whereas at pH* values >11 downfield shifts are observed. The measured pK_a value of 9.04 is assigned to a deprotonation of the HisεNH group of the imidazole ring ('pyrrole nitrogen'). The changes in chemical shifts at pH* values >11 are attributed to a deprotonation of the complexed terminal amino group.

In contrast to complex **1**, the HisεNH deprotonation in **2** occurs at much higher pH* values. In the range pH* 10.0–12.9, large (upfield) shifts for resonances of the imidazole ring protons (HisεCH: δΔ 0.49 ppm, HisδCH: 0.26 ppm) and smaller (also upfield) shifts for Gly1CH_2 (δΔ 0.01 ppm) and Gly2CH_2 (δΔ 0.01 and 0.02 ppm) were observed for **2**. The HisαCH peak showed only an upfield shift (δΔ 0.05 ppm). The small shifts seen for Gly1CH_2 and Gly2CH_2 in **2** were similar in size to shifts observed for these protons of **1** in the pH range where only HisεNH deprotonation occurs.

Deprotonations of the co-ordinated imidazole and amino groups in the gold(III) complexes were supported by the potentiometric measurements. Titration curves of $[Au^{III}(Gly\text{-}Gly\text{-}L\text{-}His\text{-}H_{-2})]Cl$ were fitted by three separated deprotonations with pK_a values of 2.58(1), 8.63(1) and 11.50(10). Taking into account the different solvent (D_2O for NMR) these values are in reasonable agreement with the NMR data and correspond to the deprotonation of the non-co-ordinated carboxylic acid and HisεNH groups, and co-ordinated amino group, respectively. Because of the low solubility of $[Pd^{II}(Gly\text{-}Gly\text{-}L\text{-}His\text{-}H_{-2})]$, the pH-metric measurements were performed only in basic solutions, and pK_a = 11.30(20) was obtained for the deprotonation of HisεNH of the imidazole ring. Deprotonation of the co-ordinated amino group of **2** could not be detected below pH 12.

Small shifts of the resonances for the histidine ring protons in $[Ni^{II}(Gly\text{-}Gly\text{-}L\text{-}His\text{-}H_{-2})]^-$ were seen above pH* 11; however, no deprotonation was observed by potentiometry.

Discussion

Crystal structures

No crystal structures of either gold(III) or palladium(II) with a tripeptide appear to have been previously reported. The bond lengths observed for **1** and **2** follow a general trend that can be deduced from crystal structures of Cu^{II} and Ni^{II} complexes of GGH derivatives. Both nickel(II) and copper(II) GGH complexes themselves are unstable towards oxygen and have not yet been crystallised. The two copper(II) structures that have previously been reported are copper(II) complexed to GGH-methyl amide (Cu^{II}GGHa)[7] and the decarboxylated copper(II)–GGH complex, α,β-didehydroglycylglycylhistaminatocopper(II) dihydrate (Cu^{II}GGHd).[36] The nickel(II) crystal structure that has previously been reported is for the decarboxylated and hydroxylated species $[Ni^{II}(Gly\text{-}Gly\text{-}\alpha\text{-}hydroxy\text{-}D,L\text{-}histamine)]\cdot 3H_2O$ (Ni^{II}GGHd).[37]

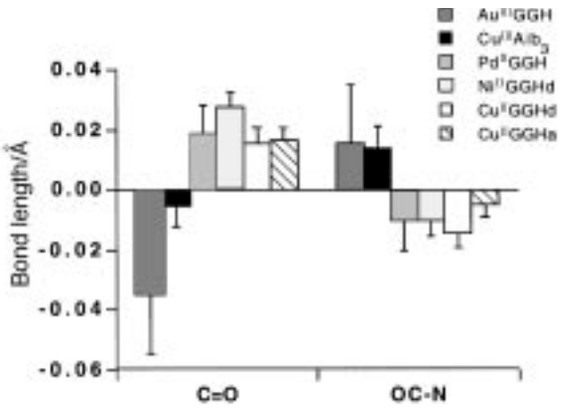

Fig. 6 Differences in the peptide bond lengths, C=O and OC–N, in various metal–chelate complexes of GGH or derivatives from peptide bond lengths in free peptides;[34] values for the copper(III) complex with tri-α-aminoisobutyric acid (Aib_3) are also shown; values are the average of two complexed peptide bonds; negative values: bonds shorter than in free peptide bond, positive values: bonds longer than in free peptide bond; one standard deviation of the bond lengths in the respective crystal structure is shown

I **II**

The bond lengths in the peptide part of the crystal structures correspond to bond lengths found in crystal structures of amino acids and peptides[34] within the experimental uncertainty of twice the standard deviation in the case of $[Pd^{II}(Gly\text{-}Gly\text{-}L\text{-}His\text{-}H_{-2})]\cdot 1.5H_2O$ and three times the standard deviation in the case of $[Au^{III}(Gly\text{-}Gly\text{-}L\text{-}His\text{-}H_{-2})]Cl\cdot H_2O$. This is also the range in which those bond lengths differ in crystal structures of various uncomplexed amino acids and peptides.[34] However, a small and possibly significant difference in bond lengths of the peptide bonds in the complex of gold(III) with GGH, compared to other metal complexes of GGH or its derivatives, is seen for the C=O bonds, which are slightly shorter in the gold(III) complex compared to free peptides, while they are slightly longer in complexes of some other metals. The reverse is observed for the amide OC–N bond. The differences in the C=O and OC–N bond lengths in metal complexes compared to the average bond length in free peptides are shown in Fig. 6 for the various metal chelate complexes of GGH and its derivatives. The values shown are the average of two complexed peptide bonds. The only crystal structure of copper(III) with a peptide-like ligand, $[Cu^{III}(H_{-2}Aib_3)]\cdot 2H_2O\cdot 1.5NaClO_4$,[9] is also included. Tri-α-aminoisobutyric acid (Aib_3) is a ligand closely related to trialanine, with additional methyl groups in place of the hydrogen atoms on the α-carbons.

It has been proposed that variations in C=O and OC–N bond lengths are linked to a preference for either of the two resonance forms (**I** or **II**) of the peptide bond.[9]

It was suggested on the basis of a comparison of bond lengths in $[Cu^{III}(H_{-2}Aib_3)]\cdot 2H_2O\cdot 1.5NaClO_4$ with bond lengths of related copper(II) and nickel(II) complexes of similar peptide ligands, that for copper(II) and nickel(II) the bond lengths of C=O and OC–N differ significantly from the values of the free peptide bond, while for copper(III), the values are equivalent to those in the free peptide bond.[9] In chelate complexes of copper(II) and nickel(II), the C=O bond was reported to lengthen and the OC–N bond to shorten due to the increased contribution of resonance form **II**, while for copper(III) it was suggested that resonance form **I** was favoured.[9] The average values of bond lengths in two complexed peptide bonds were used to establish this relationship.[9]

It can be seen from Fig. 6 that the copper(III)-complexed peptide bond lengths do differ slightly from the bond lengths in a free peptide bond to an extent comparable to other metals. However, the sign of the difference is opposite for both copper(III) and gold(III) compared to the other metals. For palladium(II), nickel(II) and copper(II), the C=O bond lengths are slightly longer and the OC–N bond lengths are slightly shorter than in the free peptide. On the contrary, for copper(III), and even more so for gold(III), the C=O bond lengths are slightly shorter and the OC–N bond lengths are slightly longer than in the free peptide. For copper(III), the different behaviour has been explained by the stronger copper(III)–nitrogen bonds, as compared to copper(II) and nickel(II), which are expected to favour resonance form **I** in which the excess electron density is resident on the peptide nitrogen.[9] The effect is somewhat more pronounced for gold(III), however, the error range of the bond lengths in this crystal structure is also larger. The stronger electron-withdrawing effect of gold(III), compared with the divalent metals mentioned above, might play a role in the preference for resonance form **I** of the peptide bond.

Trends can also be seen for the bond angles around the metal centre. The N(2)–M–N(1) and N(1)–M–N(0) angles are the ones in the two five-membered ring systems and lie well below the ideal 90° of square-planar geometry for both **1** and **2**. This is due to the strain imposed by the five-membered ring system. The bond angle formed between the amino group, the metal and the imidazole group, N(0)–M–N(34), *i.e.* the angle on the open side of the complex that does not have a chelate ring, increases in complexes of GGH and its derivatives from nickel to copper, palladium and finally gold. This parallels increases in the ionic radii of the metal ions from Ni^{II} 0.63 Å, Cu^{II} 0.71 Å, Pd^{II} 0.78 Å to Au^{III} 0.82 Å,[38] with the largest angle of 100.4° found in the structure containing the large gold(III) ion. For square-planar complexes of various metals with tetraglycine, involving metal co-ordination to the N-terminal amino group and three deprotonated peptide nitrogens, the steric constraints introduced by three linked consecutive five-membered chelate rings have been discussed by Schwederski *et al.*[39] The angle on the open side of the ring was similarly found to increase in the order $Cu^{II} < Ni^{II} < Cu^{III}$, paralleling increases in the ionic radii of the metal ions.

Reaction of GGH with $[AuCl_4]^-$

Major product **1** has identical chemical shifts to the crystallized square-planar complex $[Au^{III}(Gly\text{-}Gly\text{-}L\text{-}His\text{-}H_{-2})]^+$. The shift seen for the HisδCH proton of the intermediate **3** together with the fact that **3** shows the smallest shift for HisεCH (except minor product **5**) led to its assignment as a complex with gold(III) bound to the Hisε nitrogen.

Minor product **4** was tentatively assigned to an imidazole-bridged species consisting of the δN-bound chelate with an additional gold(III) species bound to the εN of the ring. We have shown that in the reaction of **1** with $[Au(dien)Cl]Cl_2$ (dien = diethylenetriamine), imidazole-bridged species appear at pH* values as low as 3.5.[40] The decrease in the amount of the bridged species present in the reaction mixture with increasing reaction time is most likely to be due to the decrease in pH that accompanies the reaction. The assignment is supported by the increase in the relative amount of this species in experiments carried out with a higher $[AuCl_4]^-$: GGH ratio. In these spectra it can be seen that product **4** shows inequivalent Gly2 methylene protons and a large chemical shift difference of the $His\beta CH_2$ protons, factors that are indicative of a square-planar chelate complex as will be discussed later. It has been shown that imidazole can act as a bridging ligand for Au^{III} at neutral pH.[5]

The formation of some colloidal gold during the reaction of GGH and $[AuCl_4]^-$, which was not due to the oxidation of acetate present in the reaction mixture, suggests that some of the ligand GGH is oxidized during the reaction. There are two signals in ^1H spectra obtained at the end of the monitoring period that could possibly be assigned to an unknown oxidation product **5** of GGH (Fig. 3). One is a HisεCH resonance which overlaps with the signal for the same proton of unbound ligand and the second one is a singlet in the chemical shift range of a glycine CH_2 resonance. Both of these resonances are otherwise unaccounted for and appear in similar amounts in reactions with a higher $[AuCl_4]^-$: GGH ratio (data not shown). Organic acids such as malonate are known to be oxidized by gold(III).[41]

At low pH, in the protonated cationic form, the two nitrogen donors of the imidazole ring of histidine are equivalent and can thus both act individually as binding sites for metals. The two new species appearing at the beginning of the reaction of GGH with $[AuCl_4]^-$ in similar amounts can therefore be attributed to gold(III) bound to εN or δN of the imidazole ring. Whereas one of those species eventually forms the major product of the reaction, which through X-ray crystallography is shown to be the δN-bound chelate **1**, the intermediate **3** disappears completely after a reaction time of *ca.* 23 h. The fact that no unchelated δN-bound species can be detected suggests that chelate ring-closure is very fast. Whereas gold(III) binding to the δN of histidine leads to a stable six-membered ring by deprotonation of the Gly2–His amide bond nitrogen, gold(III) binding to εN of the imidazole ring can only produce a less favourable seven-membered ring. Therefore the reaction proceeds to form eventually only the most thermodynamically stable δN-bound chelate.

A reaction displaying a biphasic behaviour has been reported for nickel and histamine at slightly acidic pH (5.8–6.6).[42] This behaviour was interpreted as arising from the parallel complexing of nickel to the two imidazole ring tautomers. While the pyridine-nitrogen-bound complex leads to the stable chelated product with nickel(II) complexed to the pyridine nitrogen and the amino group, the pyrrole-nitrogen-bound complex that formed initially dissociates in the slower step to give eventually the chelated product.[42]

pH Dependence of reaction of GGH with $[AuCl_4]^-$

It is not unexpected that the reaction is slower at a starting pH value of 1.5 compared with a starting pH value of 2.5. This is likely to be due to the suppression of the hydrolysis of $[AuCl_4]^-$ by H^+,[43] as well as to a suppression of amide deprotonation.

While in reactions of GGH with $Na[AuCl_4]$ in buffer at low pH (about 2), the major product is the square-planar chelate complex of GGH with gold(III), $[Au^{III}(Gly\text{-}Gly\text{-}L\text{-}His\text{-}H_{-2})]^+$, and a reaction intermediate is observed; reactions in buffer at pH* 4 or 5 yield an additional product, a precipitate. Apart from this precipitate, signals for free GGH and the chelated complex $[Au^{III}(Gly\text{-}Gly\text{-}L\text{-}His\text{-}H_{-2})]^+$ are also observed. The reaction is accompanied by a noticeable drop in pH. In a reaction carried out at pH* 6.5 to 7, no resonances for the chelate complex were seen and the main product of the reaction was the precipitate. It seems likely that the precipitate observed in slightly acidic and neutral solutions is a gold(III)–imidazole-bridged polymer. As mentioned above, a bridged species has been shown to form quantitatively in neutral solutions of the chelate complex of gold(III) with Gly-His.[5] In metal complexes of Gly-His, the fourth co-ordination site is free to bind to HisεN of a second chelate complex and tetramer structures have been described for complexes of gold(III) (formed at neutral pH),[5] and nickel(II) and palladium(II) (formed between pH 9 and 10).[44] We have observed that $[Au(dien)]^{3+}$ complex can co-ordinate to HisεN of $[Au^{III}(Gly\text{-}Gly\text{-}L\text{-}His\text{-}H_{-2})]^+$ at pH* values as low as 3.5.[40] A possible bridged species has also been observed in reactions of GGH and $Na[AuCl_4]$ at pH* 2; however, chelate formation was the favoured reaction at this pH value.

Thus two competing reactions between GGH and $[AuCl_4]^-$ appear to occur in aqueous solution: at low pH, only the chelate

is formed, at pH values of 4 to 5, both chelate formation and cross-linking occur while at neutral pH only cross-linking is favoured.

Reaction of GGH with $[PdCl_4]^{2-}$

The anion $[PdCl_4]^{2-}$ reacts with GGH to form the same square-planar complex at neutral pH as at pH 2, but in contrast to Au^{III} no intermediates were detected. The higher pK_a value observed for palladium(II)-induced HisεNH deprotonation suggests that palladium(II) is unlikely to form imidazole-bridged species at neutral pH.

The reaction of $[PdCl_4]^{2-}$ with Gly-His-Lys at pH 2 (1:1 peptide–metal ratio in D_2O, 300 K) has been reported to be time-dependent with the formation of a single product within about 10 h,[45] a similar time-scale as observed here. The pK_a for the palladium(II)-induced deprotonation of a peptide bond has been estimated to be below 1.5 with Gly-L-His as ligand since complete reaction occurs at pH* 2.2.[46]

The reaction of GGH with $[AuCl_4]^-$ is slow compared with other transition metals. Reactions between nickel(II) and copper(II) with GGH are fast but occur at higher pH values than reported here for gold(III) and palladium(II). Complexes of palladium(II) with peptides have been widely studied.[47] Our work shows that gold(III) is as efficient as palladium in ionizing peptide bonds at pH* values between 1 and 2.

Trends in ^{1}H chemical shifts of AuGGH, PdGGH and NiGGH

With the exception of the Hisβ protons, the ^{1}H NMR chemical shift data of the three complexes show a clear trend (Table 5). Compared to the uncomplexed ligand, the resonances of the gold complex shift downfield, whereas those for both the palladium and the nickel complex shift upfield, with the nickel complex showing very large shifts compared to the palladium complex. The β protons behave differently, with the β′ proton shifting upfield in all three complexes and the β proton shifting upfield in the nickel complex and downfield in the gold and palladium complexes. A downfield shift of the ring protons has been observed in a proposed complex of gold(III) and *N*-methylimidazole.[48]

All three chelate complexes show the characteristic additional four-bond coupling between β′H and the δ proton of the histidine ring, and inequivalent Gly2CH_2 protons. The inequivalence of the Gly2CH_2 protons is much more pronounced in the gold(III) complex than in the analogous palladium(II) and nickel(II) complexes, in which it was observed only at high field strength. Non-equivalent methylene protons have been observed previously in a complex of palladium(II) with the dipeptide Ala-Gly in which the carboxylate group was unbound.[49]

HisεNH deprotonation

The pH titration (Fig. 5) of $[Au^{III}(Gly\text{-}Gly\text{-}L\text{-}His\text{-}H_{-2})]Cl\cdot H_2O$ **1** shows shifts on all but the N-terminal Gly1CH_2 protons for a titrating group with a pK_a < 5 (pK_a = 2.58 ± 0.01 measured by potentiometry) which can be attributed to the carboxyl group, confirming that the carboxylate group is not complexed to gold(III) in solution either.

A second titrating group in **1** with a pK_a value of 9.04 ± 0.01 (8.63 ± 0.01 by potentiometry) was assigned to the deprotonation of the uncomplexed HisεNH proton ('pyrrole nitrogen') which usually shows a pK_a value of 14.2–14.6.[16] Deprotonation of this group ('pyrrole nitrogen') through across-the-ring-ionization by a metal attached to the HisδN has been reported before, but for most metals the pK_a values reported are well above 10. However, deprotonation of the 'pyrrole nitrogen' with a lower pK_a value was found for some trivalent metal complexes: cobalt(III) in aquocobalamin complexed to imidazole (pK_a = 9.6),[50] and pentaammineruthenium(III) complexed to imidazole[51] (pK_a = 8.9) and histidine[52] (pK_a = 8.7). Likewise, the complexation of methylmercury(II) to imidazole gives rise to a pK_a value of 9.6 for the deprotonation of the 'pyrrole nitrogen'.[53] Reactions of $[Au(dien)Cl]^{2+}$ with GGH confirm the low pK_a value for HisεNH deprotonation in $[Au^{III}(Gly\text{-}Gly\text{-}L\text{-}His\text{-}H_{-2})]^+$ reported here.[40]

Deprotonation of the metal-complexed terminal amino group in a complex of GGH with copper(III) has been reported[54] and a pK_a value of 8.2 ± 0.1 was determined for this process, but curiously, no deprotonation of HisεNH in the complex was detected.

In contrast to the gold(III) complex, $[Pd^{II}(Gly\text{-}Gly\text{-}L\text{-}His\text{-}H_{-2})]$ shows deprotonation of HisεNH only above pH* 10. The pK_a value of 11.3 ± 0.2 determined for $[Pd^{II}(Gly\text{-}Gly\text{-}L\text{-}His\text{-}H_{-2})]$ by potentiometry is in a similar range to the value of 10.83 reported for the same process in $[Pd(en)(His)]^+$ (en = ethane-1,2-diamine) where histidine co-ordination was suggested to be *via* the N-terminal amino group and HisδN.[49]

The pK_a value of 8.63 ± 0.01 reported here that was determined by potentiometry for $[Au^{III}(Gly\text{-}Gly\text{-}L\text{-}His\text{-}H_{-2})]^+$ is the lowest value measured so far for any metal for HisεNH deprotonation by across-the-ring ionization and illustrates the strong electron-withdrawing power of gold(III).

Acknowledgements

This work was supported by the Wellcome Trust (Toxicology Studentship to S. L. B., Ref. No. 035931/Z/92/Z), the Royal Society and the BBSRC. We thank the University of London Intercollegiate Research Service and the Medical Research Council Biomedical Centre for the provision of NMR facilities.

References

1 D. Schuhmann, M. Kubicka-Muranyi, J. Mirtschewa, J. Günther, P. Kind and E. Gleichmann, *J. Immunol.*, 1990, **145**, 2132.
2 J. Verwilghen, G. H. Kingsley, L. Gambling and G. S. Panayi, *Arthritis Rheum.*, 1992, **35**, 1413.
3 B. Beverly and D. Couri, *Fed. Proc.*, 1987, **46**, 854; C. F. Shaw, III, S. Schraa, E. Gleichmann, Y. P. Grover, L. Dunemann and A. Jagarlamudi, *Metal Based Drugs*, 1994, **1**, 351.
4 A. A. Isab and P. J. Sadler, *Biochim. Biophys. Acta*, 1977, **492**, 322; C. F. Shaw, III, M. P. Cancro, P. L. Witkiewicz and J. E. Eldridge, *Inorg. Chem.*, 1980, **19**, 3198; W. E. Smith and J. Reglinski, *Perspect. Bioinorg. Chem.*, 1991, **1**, 183; G. Natile, E. Bordignon and L. Cattalini, *Inorg. Chem.*, 1976, **15**, 246.
5 M. Wienken, B. Lippert, E. Zangrando and L. Randaccio, *Inorg. Chem.*, 1992, **31**, 1983.
6 H. C. Freeman, *Adv. Protein Chem.*, 1967, **22**, 257.
7 N. Camerman, A. Camerman and B. Sarkar, *Can. J. Chem.*, 1976, **54**, 1309.
8 H. C. Freeman, J. M. Guss and R. L. Sinclair, *Acta Crystallogr., Sect. B*, 1978, **34**, 2459.
9 L. L. Diaddario, W. R. Robinson and D. W. Margerum, *Inorg. Chem.*, 1983, **22**, 1021.
10 M. Sabat, K. A. Satyshur and M. Sundaralingam, *J. Am. Chem. Soc.*, 1983, **105**, 976.
11 B. T. Khan, S. Shamsuddin and K. Venkatasubramanian, *Polyhedron*, 1992, **11**, 671.
12 M. Wienken, E. Zangrando, L. Randaccio, S. Menzer and B. Lippert, *J. Chem. Soc., Dalton Trans.*, 1993, 3349.
13 H. C. Freeman and M. L. Golomb, *Chem. Commun.*, 1970, 1523.
14 T. G. Appleton, J. R. Hall, T. W. Hambley and P. D. Prenzler, *Inorg. Chem.*, 1990, **29**, 3562.
15 H. Sigel and R. B. Martin, *Chem. Rev.*, 1982, **82**, 385.
16 G. Yagil, *Tetrahedron*, 1967, **23**, 2855; R. J. Sundberg and R. B. Martin, *Chem. Rev.*, 1974, **74**, 471.
17 R. B. Martin, *Metal Ions Biol. Syst.*, 1979, **9**, 1.
18 H. Aiba, A. Yokoyama and H. Tanaka, *Bull. Chem. Soc. Jpn.*, 1974, **47**, 1437.
19 P. J. Morris and R. B. Martin, *J. Am. Chem. Soc.*, 1970, **92**, 1543.
20 I. Sóvágó, T. Kiss and A. Gergely, *J. Chem. Soc., Dalton Trans.*, 1978, 964.
21 T. Sakurai and A. Nakahara, *Inorg. Chem.*, 1980, **19**, 847.
22 J. L. Markley, *Acc. Chem. Res.*, 1975, **8**, 70.
23 KALEIDAGRAPH, Synergy Software, Reading, PA, 1994.

24 G. F. Bryce, R. W. Roeske and F. R. N. Gurd, *J. Biol. Chem.*, 1966, **241**, 1072.
25 R. W. Hay, M. M. Hassan and C. Yoy-Quan, *J. Inorg. Biochem.*, 1993, **52**, 17.
26 F. P. Bossu and D. W. Margerum, *Inorg. Chem.*, 1977, **16**, 1210.
27 H. M. Irving, L. G. Miles and L. D. Pettit, *Anal. Chim. Acta*, 1967, **38**, 475.
28 L. Zekany and I. Nagypal, in *Computational Methods for the Determination of Stability Constants*, ed. D. Leggett, Plenum, New York, 1985.
29 N. Walker and D. Stuart, *Acta Crystallogr., Sect. A*, 1983, **39**, 158.
30 G. M. Sheldrick, SHELXS 86, Program for the Solution of Crystal Structures, University of Göttingen, 1986.
31 G. M. Sheldrick, SHELXL 93, Program for Crystal Structure Determination, University of Göttingen, 1993.
32 H. D. Flack, *Acta Crystallogr., Sect. A*, 1983, **39**, 876.
33 S. Karaulov, SNOOPI, Molecular Plotting Program, University of Wales, Cardiff, 1992.
34 R. E. Marsh and J. Donohue, *Adv. Protein Chem.*, 1967, **22**, 235.
35 K. Wüthrich, *NMR of Proteins and Nucleic Acids*, Wiley, New York, 1986, pp. 23–25.
36 P. de Meester and D. J. Hodgson, *Inorg. Chem.*, 1978, **17**, 440.
37 W. Bal, M. I. Djuran, D. W. Margerum, E. T. Gray, jun., M. A. Mazid, R. T. Tom, E. Nieboer and P. J. Sadler, *J. Chem. Soc., Chem. Commun.*, 1994, 1889.
38 R. D. Shannon, *Acta Crystallogr., Sect. A*, 1976, **32**, 751.
39 B. E. Schwederski, H. D. Lee and D. W. Margerum, *Inorg. Chem.*, 1990, **29**, 3569.
40 S. L. Best, Ph.D. Thesis, University of London, 1996.
41 B. S. Maritz and R. van Eldik, *Inorg. Chim. Acta*, 1976, **20**, 43.
42 P. Dasgupta and R. B. Jordan, *Inorg. Chem.*, 1985, **24**, 2721.
43 N. Bjerrum, *Bull. Soc. Chim. Belg.*, 1948, **57**, 432.
44 P. J. Morris and R. B. Martin, *J. Inorg. Nucl. Chem.*, 1971, **33**, 2913.
45 J.-P. Laussac, M. Pasdeloup and N. Hadjiliadis, *J. Inorg. Biochem.*, 1987, **30**, 227.
46 D. L. Rabenstein, A. A. Isab and M. M. Shoukry, *Inorg. Chem.*, 1982, **21**, 3234.
47 See, L. D. Pettit and M. Bezer, *Coord. Chem. Rev.*, 1985, **61**, 97; S. Kasselouri, A. Garoufis, M. Lamera-Hadjiliadis and N. Hadjiliadis, *Coord. Chem. Rev.*, 1990, **104**, 1.
48 D. J. Radanovic, Z. D. Matovic, G. Ponticelli, P. Scano and I. A. Efimenko, *Transition Met. Chem.*, 1994, **19**, 646.
49 T. P. Pitner, E. W. Wilson and R. B. Martin, *Inorg. Chem.*, 1972, **11**, 738.
50 W. J. Eilbeck and M. S. West, *J. Chem. Soc., Dalton Trans.*, 1976, 274.
51 R. J. Sundberg, R. F. Bryan, I. F. Taylor and H. Taube, *J. Am. Chem. Soc.*, 1974, **96**, 381.
52 R. J. Sundberg and G. Gupta, *Bioinorg. Chem.*, 1973, **3**, 39.
53 C. A. Evans, D. L. Rabenstein, G. Geier and I. W. Erni, *J. Am. Chem. Soc.*, 1977, **99**, 8106.
54 M. R. McDonald, W. M. Scheper, H. D. Lee and D. W. Margerum, *Inorg. Chem.*, 1995, **34**, 229.

Received 27*th February* 1997; *Paper* 7/01395G